

Ligand-protein interactions in lysozyme investigated through a dual-resolution model

Raffaele Fiorentini,¹ Kurt Kremer,¹ and Raffaello Potestio^{2,3,*}

¹*Max Planck Institute for Polymer Research, Mainz, Germany*

²*Physics Department, University of Trento, via Sommarive, 14 I-38123 Trento, Italy*

³*INFN-TIFPA, Trento Institute for Fundamental Physics and Applications, I-38123 Trento, Italy*

(Dated: February 19, 2020)

A fully atomistic modelling of biological macromolecules at relevant length- and time-scales is often cumbersome or not even desirable, both in terms of computational effort required and a *posteriori* analysis. This difficulty can be overcome with the use of multi-resolution models, in which different regions of the same system are concurrently described at different levels of detail. In enzymes, computationally expensive atomistic detail is crucial in the modelling of the active site in order to capture e.g. the chemically subtle process of ligand binding. In contrast, important yet more collective properties of the remainder of the protein can be reproduced with a coarser description. In the present work, we demonstrate the effectiveness of this approach through the calculation of the binding free energy of hen egg white lysozyme (HEWL) with the inhibitor di-N-acetylchitotriose. Particular attention is posed to the impact of the mapping, i.e. the selection of atomistic and coarse-grained residues, on the binding free energy. It is shown that, in spite of small variations of the binding free energy with respect to the active site resolution, the separate contributions coming from different energetic terms (such as electrostatic and van der Waals interactions) manifest a stronger dependence on the mapping, thus pointing to the existence of an optimal level of intermediate resolution.

I. INTRODUCTION

One of the most relevant challenges of computational biochemistry and biophysics is the accurate calculation of binding free energies [1–3], which represents one of the key steps in the identification of pharmacological targets as well as in the development of new drugs [4–6]. However, the large sizes of the molecules under examination (often above the hundred of residues), as well as the necessity to screen through large datasets of potential candidate molecules, make this effort onerous in terms of time and computational resources.

A promising way to mitigate these limitations is the use of multiple-resolution models of the protein, that is, representations in which different parts of the molecule are concurrently described at different levels of resolution [7–15]. The chemically relevant part of the protein, e.g. the active site, is modelled at level of detail, typically atomistic. For the remainder, on the contrary, a simplified representation is used, where several atoms are lumped together in effective interaction sites. The working hypothesis underlying these methods is that only a relatively small part of the molecule requires an explicitly atomistic treatment; the remainder, in fact, is mainly responsible for large-scale, collective fluctuations whose function-oriented role is well recognised and prominent [15–19], however also prone to be accurately reproduced by lower-resolution representations [20–25]. Hence, the resulting model favourably joins the accuracy of an atomistic (AT) description where needed and the computational efficiency of a coarse-grained (CG) one where possible.

In order to take full advantage of the dual-resolution approach to protein modelling, though, one has to solve a few key open issues: first, the definition of the appropriate coarse-grained model to employ in the low-resolution part [25–33]; second, the coupling between high- and low-resolution models, which has to be performed so as to guarantee that the appropriate observables are reproduced with respect to the reference provided for example by a fully atomistic simulation. This issue entails a further one, namely the identification of the correct observables apt to quantify the fidelity with which the behaviour of the system is reproduced by the dual-resolution model; third, the selection of the subpart of the molecule that *requires* a high-resolution modelling. In the present work we will focus specifically on this third aspect.

Various methods and approaches have been developed in the past few years to describe proteins in dual resolution [7, 10–14]. In general, the high-resolution part is modelled at the all-atom level, making use of one of the several atomistic force fields available. The coarse-grained representations range from simple bead-spring elastic networks [15, 20, 23] to more sophisticated Gō-type models [11]. Recently, we have proposed a dual-resolution model [15] where, in the CG part, only the C_α carbons of the protein chain are retained and connected one with the other by harmonic bonds. This model has been employed in the present work with the aim of assessing the accuracy of a hybrid atomistic/coarse-grained description of a protein for binding free energy calculations. The system under examination is hen egg-white lysozyme in explicit water, bound to a sugar substrate, di-N-acetylchitotriose. We carried out calculations of the binding free energy of the ligand in the active site, with a twofold objective. In fact, not only we aimed at verifying

* raffaello.potestio@unitn.it

that the computed quantity in the dual-resolution model matches a reference, all-atom calculation; but rather we also investigated the impact of different choices in the definition of the high-resolution subdomain. This aspect bears the highest prominence, as it is becoming increasingly more evident that a crucial component in the construction of accurate and effective low-resolution models for biological and soft matter systems is represented by the mapping [15, 32, 33], that is, the particular selection of collective variables employed to describe the system. Here, we provide novel evidence of this general property in the context of a dual-resolution model of a biomolecule, and describe a transferable strategy to tackle this issue.

II. METHODS

The system under examination in the present work is hen egg-white lysozyme (HEWL) in aqueous solution. In this model, the binding site of the enzyme and the substrate molecule, the inhibitor di-N-acetylchitotriose, are represented with atomistic detail. The protein model employed is not adaptive, that is, the resolution of a given residue is fixed –either atomistic or coarse-grained– and does not change throughout a simulation. However, at difference with other works [8, 9, 11], several values of the number of protein residues treated at high resolution have been explored and employed in independent calculations. The impact of choosing different numbers of active site residues to model at the atomistic level is a central aspect of this study. The coarse-grained model employed to describe the low-resolution part of the protein is a simple bead-spring representation where the selected sites (namely the C_α atoms) are connected by elastic bonds penalising the deviations from the distances that interacting atoms have in the reference conformation. Two values of elastic constants employed, one for C_α 's along the chain, and one for all other bonds. Water molecules are described in atomistic detail throughout the whole simulation box: the interaction with the high-resolution part of the protein takes place through the standard all-atom force field, while the interaction with the coarse-grained beads is mediated by a purely repulsive potential acting on the sole oxygen atom.

Hereafter we provide a detailed description of the model. We first discuss the calculation of the binding free energy ΔG_{bind} , then we outline the dual-resolution model and its coupling to the atomistic part, and finally report information about the simulation setup. Further details are made available in the *Supporting Information*.

A. Binding Free Energy calculation

One of the key points of this work is the calculation of the protein-ligand binding free energy ΔG_{bind} , which quantifies the affinity of a molecule towards a protein [1–3]. As such, it plays a prominent role in the investigation

of the biochemical function and activity of enzymes and similar biomolecules, and in the development of effective drugs.

ΔG_{bind} is defined as the difference between the free energy of the system in the configuration in which the ligand is bound to the active site (G_b) and the corresponding value when the ligand is absent (G_{ub}):

$$\Delta G_{bind} = G_b - G_{ub} \quad (1)$$

This value, in the specific case under examination, varies according to the number of active site residues modelled with atomistic resolution, as we will see in Sect. III.

The free energy difference between two states is here computed by means of thermodynamic integration (TI) [34]. Specifically, a scalar $\lambda \in [0, 1]$ is defined which parametrises the potential energy of the system as $U_\lambda(\mathbf{r}) = \lambda U_A(\mathbf{r}) + (1 - \lambda)U_B(\mathbf{r})$ connecting the states A and B. The sought quantity is given by:

$$\Delta G = \int_0^1 \left\langle \frac{\partial U(\lambda)}{\partial \lambda} \right\rangle_\lambda d\lambda \quad (2)$$

Since the free energy is a state function, the nature of the path is unimportant, and one can choose a thermodynamic cycle that connects the bound and unbound states through several intermediate ones, as illustrated in Fig.1. In particular, we can identify two main terms: the insertion of the ligand from vacuum to water ΔG_{lig} , and the decoupling from the protein ΔG_{compl} . A further step is the removal of the restraints that keep the ligand in proximity of the protein during the damping of the ligand-protein interactions, $\Delta G_{r.off}$; this latter calculation can be carried out analytically without the need to run simulations. Hence, ΔG_{bind} is the algebraic sum of the previous three terms:

$$\Delta G_{bind} = \Delta G_{compl} + \Delta G_{lig} + \Delta G_{r.off} \quad (3)$$

According to the previous definitions of each term, neither ΔG_{lig} nor $\Delta G_{r.off}$ changes with the protein resolution: indeed, the former corresponds to the solvation free energy of the ligand, which is always treated at the atomistic level; likewise, the calculation of the restraint removal free energy is analytic [3]. The unique term that varies depending on the number of active site residues modelled in high resolution is the free energy change of the protein-ligand complex between the bound state and the state where the ligand is removed, that is, the variation of ΔG_{bind} is equal to the variation of ΔG_{compl} .

The alchemical change in the calculation of ΔG_{compl} is performed in three steps (in the following, the subscripts c and ℓ stand for complex and ligand, respectively). First, one adds a set of restraints between protein

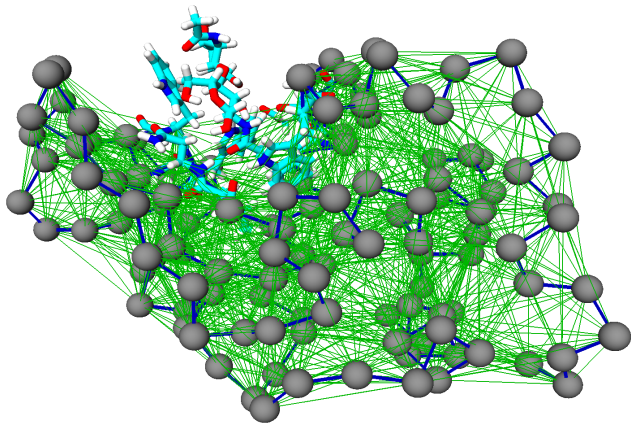


FIG. 2: Visualisation of the dual-resolution protein [15]. The residues included in atomistic detail are shown in red, blue, cyan and white (O, N, C and H atoms). The grey spheres are ENM nodes, the stiff backbone springs are shown as dark blue lines and all others (weaker) springs are shown in green.

residues to be described at the atomistic level, we sorted them by increasing distance of their the center of mass from the closest ligand atom.

The water-CG protein interaction consists in a simple excluded volume, modelled *via* a Weeks-Chandler-Anderson (WCA) potential [35]. The details about the procedure followed to determine the ENM elastic constants and the excluded volume interaction are provided in the *Supporting Information*, while the numerical values of the resulting parameters are reported hereafter.

C. Simulation details

The reference model is given by the 2 ns equilibrated PDB structure 1HEW in the NPT ensemble (the Parrinello-Rahman barostat [36] with a time constant of 2.0 ps and 1 bar was used). Both fully atomistic and dual-resolution models of HEWL are solvated in water and placed in a cubic simulation box of 7.06 nm side. The force field employed is Amber99SB [37], whereas the water model is TIP3P [38]. The inhibitor, which was always atomistic, had GLYCAM forcefield parameters consistent with Amber99SB [39]. The TI binding free energy calculation consists of 3 different steps: ΔG_{compl} , $\Delta G_{r.off}$, ΔG_{lig} :

1. The protein-ligand complex free energy (ΔG_{compl}) calculation uses 11 λ values per $\Delta G_{restr.on,c}$, 5 evenly spaced λ values per $\Delta G_{LJ,c}$ (with separation 0.20) and 15 λ values per $\Delta G_{coul,c}$, with 600 ps of simulation per λ in the fully atomistic case, and 4000 ps in the dual-resolution case to improve the statistics.

2. The restraint removal free energy ($\Delta G_{r.off}$) calculation is analytical (details on *Supporting Information*).
3. The ligand solvation free energy (ΔG_{lig}) calculation uses 5 evenly spaced λ values per $\Delta G_{coul,\ell}$ (with separation 0.20) and 16 λ values per $\Delta G_{LJ,\ell}$, with 600 ps of simulation of each λ -value.

In the thermodynamic integration we employ the soft-core potential of Ref. [40] with parameters $\alpha = 0.5$ and $p = 1.0$ to avoid possible singularities in the Lennard-Jones terms from atoms overlapping during the alchemical change. The temperature is kept constant at 298 K by means of a Langevin thermostat with a friction constant $\gamma = 15 \text{ ps}^{-1}$. The integration step is 1 fs. The calculation of electrostatic interaction is performed using the reaction field method with a dielectric constant $\epsilon = 80$ and a cutoff of 1.2 nm. These parameters are a good compromise between speed and accuracy, as verified in Ref. [41]. The SETTLE [42] and RATTLE [43] algorithms for rigid water and rigid bonds to hydrogen have been used. Each system is prepared using fully atomistic minimisation with steepest descent and 6 ns of equilibration in NVT (for both ligand-free and ligand-bound systems). All simulations (both fully atomistic and dual-resolution) are carried out with the ESPResSo++ simulation package [44, 45], in which we have implemented TI (except in case of annihilation, for which all steps are performed in both ESPResSo++ and GROMACS [46]). Some preliminary fully atomistic equilibration simulations use GROMACS. The error bars shown are calculated using the Student t at 95% confidence limit [47], via standard deviations obtained using block averaging in which all trajectories are divided into four blocks of equal length.

The parametrization of the dual-resolution model is consistent with the work in Ref.[15]: the spring constant between consecutive C_α nodes along the backbone (k_b) has a stiff value of $5 \cdot 10^4 \text{ kJ} \cdot \text{mol}^{-1} \cdot \text{nm}^{-2}$, whilst all the other ones (k_{nb}) have a value of $160 \text{ kJ} \cdot \text{mol}^{-1} \cdot \text{nm}^{-2}$, until 1.2 nm as cutoff, parametrised by minimising the average root mean square error in the C_α RMSF. Moreover, a WCA interaction is applied between C_α nodes and all solvent molecules center of mass. In the WCA potential, ϵ has a value of $0.34 \text{ kJ} \cdot \text{mol}^{-1}$ arbitrarily chosen as the value for carbon in the atomistic forcefield, and $\sigma_i = R_{g,i} \cdot c$ where $R_{g,i}$ is the radius of gyration of a given residue i where c is the same for all amino acids. The value of c is tuned to give the correct bulk water density of reference for a protein-water system. The c value found is 0.658. Further explanations about c can be found in the *Supporting Information*.

III. RESULTS AND DISCUSSION

We performed the calculation of ΔG_b of lysozyme modelled in dual-resolution, varying the number of atomistic residues constituting the binding site and comparing the

results with a fully atomistic reference simulation. Recall that the binding free energy calculation consists of three steps: restraint removal, ligand ΔG , and ligand-complex ΔG ; of these, only the latter depends on protein resolution, that is, only ΔG_{compl} assumes different values for different numbers of active site residues described at the all-atom level.

As explained in the previous section, the contribution coming from the restraints can be analytically computed and amounts to $\Delta G_{r_off} = -31.3 \text{ kJ} \cdot \text{mol}^{-1}$. Likewise, the Coulomb and Lennard-Jones contributions to the ligand free energy ΔG_{lig} are the following:

$$\begin{aligned}\Delta G_{coul,\ell} &= -142.8 \pm 1.7 \text{ kJ} \cdot \text{mol}^{-1} \\ \Delta G_{LJ,\ell} &= -9.1 \pm 6.3 \text{ kJ} \cdot \text{mol}^{-1}\end{aligned}$$

Hence:

$$\Delta G_{lig} = -151.9 \pm 8.0 \text{ kJ} \cdot \text{mol}^{-1}$$

The final step is the calculation of ΔG_{compl} , whose results, including the comparison between dual-resolution model and fully atomistic reference, are shown in Tab. II and illustrated in Fig. 3.

The first three columns of the table describe the Coulomb, Lennard-Jones, Restraints contributions to free energy, respectively, while the last one corresponds to the value of the total ligand-protein complex free energy. All the values are expressed in $\text{kJ} \cdot \text{mol}^{-1}$. In Fig. 3, the atomistic reference is represented with a dash black line with its error bar. In particular, panels (a), (b) and (c) show the three components that contribute to the total complex free energy, reported in panel (d). Looking at these values as a function of the number of all-atom active site residues, we notice that there are important deviations of the free energy from the reference, especially in the case of 3 and 4 atomistic residues. On the contrary, the total value of the binding free energy agrees with the reference within the error bar in all cases.

Furthermore, we observe that the trend of free energy values, in comparison to the reference, is essentially the same: starting from 3 amino acids it approaches the reference until reaching 6, both in its components and in total. In contrast, going from 6 to 8 atomistic residues the value deviates from the reference, even though the total remains close to it. Finally, from 8 to 10, ΔG converges again. Hence, increasing the number of atomistic residues does not introduce necessarily an improvement of the computed free energy, at least as long as the various free energy components are considered separately.

In order to gain further, quantitative insight into these results, we computed the the quadratic deviation from the reference, δ^2 , defined as:

$$\begin{aligned}\delta_i^2 &= \delta_{i-Coul}^2 + \delta_{i-LJ}^2 + \delta_{i-Restr}^2 = \\ &= (\Delta G_{Coul,i} - \Delta G_{Coul-at})^2 \\ &+ (\Delta G_{LJ,i} - \Delta G_{LJ-at})^2 \\ &+ (\Delta G_{Restr,i} - \Delta G_{Restr-at})^2\end{aligned}\quad (5)$$

where the index $i = 3 \dots 10$ runs over atomistic residues.

Fig. 4 reports δ^2 as a function of the number of active site amino acids modelled with atomistic detail.

The plot shows that the binding free energy computed in the dual-res model approaches the reference as the number of atomistic active site residues increases, and most importantly this approach takes place for each component up to 6 residues. Beyond this value, though, the trend stops and the deviation becomes larger, peaking at 8 residues and decreasing when further atomistic amino acids are added. These results highlight a non-monotonic dependence of the free energy on the mapping, that is, the number of retained atomistic residues. If, on the one hand, the overall value of the binding free energy (Fig. 3 panel d) levels to the reference with as few all-atom residues as 4, the separate components oscillate and reach the plateau only for larger numbers. The existence of a minimum in the standard deviation of all three contributions pinpoints a particular number of atomistic active site residues for which the accuracy of the computed free energy is the highest and the economy of the high-resolution subpart the largest. Including more than 6 atomistic residues counterintuitively worsens the result –when the various contributions are looked at– and the previous accuracy is only recovered when more residues are included. This behaviour suggests that the total free energy undergoes an error cancellation which hides the deviations of the separate terms.

A possible explanation for this nontrivial behaviour is that when 6 active site residues are modelled with all-atom accuracy (Fig. 5b) the ligand is stable in the catalytic site, namely it is surrounded by a complete shell of atomistic residues. The addition or deletion of other residues (Figs. 5c and 5a respectively) leads to a worsening of ΔG : in the first case, the two added residues (in pink and grey) are located behind the first shell of amino acids (far away from the ligand) and start to form a second, incomplete shell; in the second case, only three atomistic amino acids take part in the direct interaction with the ligand: therefore, the first layer is still incomplete and important interactions are missing; in order to improve the free energy value one has to add further amino acids in order to complete the second shell. We emphasise that the impact on the deviation from the reference is inversely proportional to the distance of the added/removed amino acid. Thus, the farther the atomistic amino acid is from the ligand, the more negligible its effect is. In the *Supporting Information* we provide detail about the other numbers of all-atom residues not reported here. Finally, the values of binding free energy (also for the case of annihilation whose calculations are reported in the *Supporting Information*) are summarised in Tab. III and illustrated in Fig. 6.

TABLE II: In this table are reported the resulting values of free energy of Complex Free Energy (4th column) and its components (Coulomb, Lennard Jones and Restraints respectively in the first three columns) in fully atomistic system and varying the number of atomistic residues. All the values are in $kJ \cdot mol^{-1}$ and performed with Thermodynamic Integration. Moreover, all simulations are carried out in ESPResSo++. In particular, for each value of λ , the dual-resolution simulations with different number of atomistic residues last 4 nsec; the atomistic simulation, instead, lasts 0.6 ns (600 ps)

at res	$\Delta G_{\text{Coul,c}}$	$\Delta G_{\text{LJ,c}}$	$\Delta G_{\text{Restr_on,c}}$	ΔG_{compl}
fully-at	145.2 ± 3.5	44.2 ± 5.2	3.6 ± 0.4	193.0 ± 9.1
aa-3	125.5 ± 7.0	50.4 ± 6.3	8.3 ± 1.1	184.2 ± 14.4
aa-4	141.4 ± 4.9	39.7 ± 9.4	7.2 ± 1.0	188.3 ± 15.3
aa-5	140.2 ± 2.8	48.7 ± 4.5	7.5 ± 1.2	196.4 ± 8.5
aa-6	147.0 ± 1.9	41.7 ± 5.4	5.1 ± 0.5	193.8 ± 7.8
aa-7	144.5 ± 0.8	38.4 ± 3.8	5.0 ± 0.2	187.9 ± 4.8
aa-8	148.0 ± 1.4	33.6 ± 1.9	6.4 ± 1.8	188.0 ± 5.1
aa-9	143.4 ± 4.7	38.1 ± 5.3	5.1 ± 0.3	186.6 ± 10.3
aa-10	145.9 ± 2.2	38.2 ± 1.0	4.4 ± 0.3	188.5 ± 3.5

IV. CONCLUSIONS

In this work we have shown how the dual resolution model employed, constituted by an all-atom subregion coupled to an elastic network model remainder, can be used to calculate the binding free energy of an enzyme-substrate complex with atomistic accuracy. Furthermore, and most importantly, we have highlighted the impact that different choices of the model resolution can have. Specifically, we have computed the total value of the binding free energy as well as that of its various energetic components, and quantitatively inspected how these change when different selections are performed for the subgroup of amino acids, ranging from 3 to 10 in total, to be modelled at the fully atomistic level.

At first sight, one can appreciate that the binding free energy value rapidly converges to the atomistic reference when as few as 4 amino acids constituting the active site are described all-atom. This comforting result, however, unveils a greater complexity when the different terms constituting the free energy are looked at separately. These show an oscillating behaviour as the number of all-atom residues in the active site is increased, with a decreasing difference from the reference followed by a sudden jump to larger values, which dampens upon further addition of atomistic amino acids. The rationale in this behaviour is identified in the structure of the active site, which is constituted by a first shell of the six residues exposed to the solvent and closest to the ligand;

when further amino acids beyond these are modelled with atomistic resolution, they interact with the substrate affecting the binding free energy components and shifting them away from the reference, with a steadily lowering impact as the model’s resolution is increased - as one can expect. Surprisingly, very little if no signal of this behaviour is observed in the value of the binding free energy as a whole, rather it becomes visible only upon inspection of its separate contributions.

The results of this work thus highlight the importance of mapping in the construction of multi-scale and multi-resolution models, as a higher degree of detail does not necessarily correlate with a higher accuracy of the quantities of interest. The implications of these observations should serve as a warning in the realisation of coarse-grained models concurrently employing various levels of detail for different regions of the same system, whose range of application spans from fundamental understating of a molecule’s properties to real-life pharmaceutical applications.

ACKNOWLEDGMENTS

The authors are grateful to Robinson Cortes-Huerto and Thomas Tarenzi for a critical reading of the manuscript. This project has received funding from the European Research Council (ERC) under the European Unions Horizon 2020 research and innovation programme (grant agreement no. 758588-VARIAMOLS and grant agreement no. 340906-MOLPROCOMP).

-
- [1] Boyce SE, Mobley DL, Rocklin GJ, Graves AP, Dill KA, and Shoichet BK. Predicting ligand binding affinity with alchemical free energy methods in a polar model binding site. *J Mol Bio.*, page 747763, 2009.
- [2] Aldeghi M., Bluck J.P., and Biggin P.C. Absolute al-

chemical free energy calculations for ligand binding: A beginners guide. *Computational Drug Discovery and Design*, 1762:199–232, 2018.

- [3] Stefan Boresch, Franz Tetteringer, Martin Leitgeb, and Martin Karplus. Absolute binding free energies: A quan-

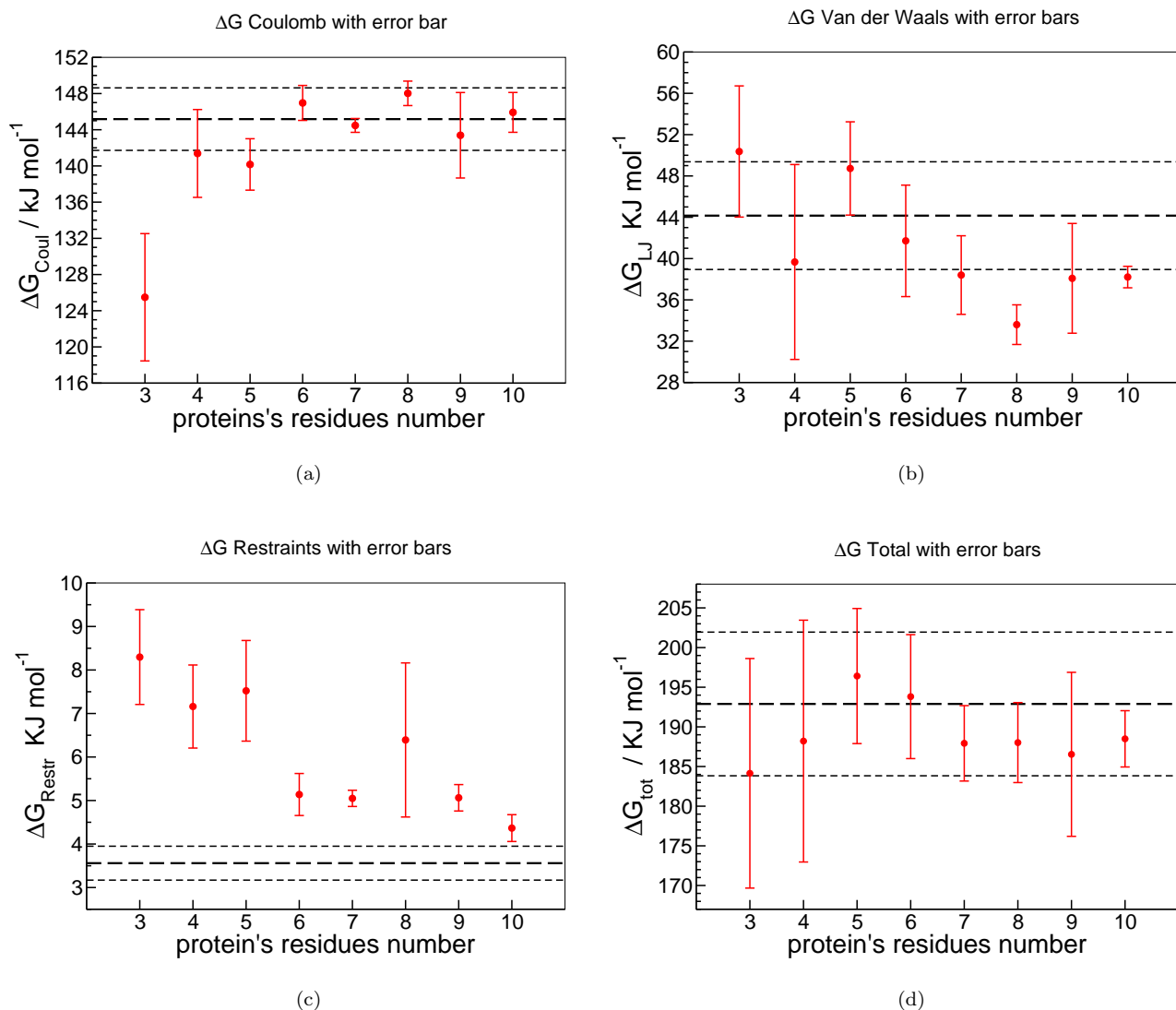


FIG. 3: (a) Coulomb, (b) Lennard-Jones, (c) restraint and (d) total free energies in the protein-ligand complex, as a function of protein's residues number included in atomistic detail in the multi-resolution set-up. The heavy dashed black horizontal lines are the reference values from fully atomistic simulations, and the lighter dotted black horizontal lines are the error bars for those values. These simulations use decoupling, not annihilation. y-axes do not cover the same energy range.

- titative approach for their calculation. *J. Phys. Chem. B*, 107(35):9535–9551, 2003.
- [4] Zoe Cournia, Bryce Allen, and Woody Sherman. Relative binding free energy calculations in drug discovery: Recent advances and practical considerations. *Journal of Chemical Information and Modeling*, 57(12):2911–2937, 2017. PMID: 29243483.
- [5] Robert Abel, Lingle Wang, Edward D. Harder, B. J. Berne, and Richard A. Friesner. Advancing drug discovery through enhanced free energy calculations. *Accounts of Chemical Research*, 50(7):1625–1632, 2017. PMID: 28677954.
- [6] B. N. Dominy. Molecular recognition and binding free energy calculations in drug development. *Current Pharmaceutical Biotechnology*, 9(2):87–95, 2008.
- [7] Cameron F. Abrams, Luigi Delle Site, and Kurt Kremer. Dual-resolution coarse-grained simulation of the bisphenol-*a*-polycarbonate/nickel interface. *Phys. Rev. E*, 67:021807, Feb 2003.
- [8] Raffaello Potestio, Christine Peter, and Kurt Kremer. Computer simulations of soft matter: Linking the scales. *Entropy*, 16(8):4199–4245, 2014.
- [9] Raffaele Fiorentini, Kurt Kremer, Raffaello Potestio, and Aoife Fogarty. Using force-based adaptive resolution simulations to calculate solvation free energies of amino acid sidechain analogues. *The Journal of Chemical Physics*, 146:244113, 06 2017.
- [10] Richard J. Gowers and Paola Carbone. A mul-

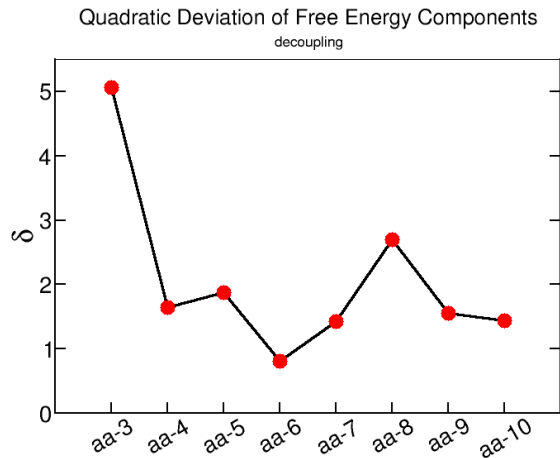


FIG. 4: Square root of quadratic deviation δ^2 vs the number of atomistic residues chosen. The plot shows that in the case of 6 atomistic residues, the value of quadratic deviation is the lowest one and hence it means that such a number leads the best result of free energy. Moreover the black line shows the trend of FE values as discussed in the section III

TABLE III: Representation of Free Energies values computed in ESPResSo++ and GROMACS (respectively *espp* and *grom* using a short notation on the table) in case of annihilation and decoupling. The table is divided in three column: from left to right are represented the ligand, protein-ligand complex and binding FE. The latter is the algebraic sum of ΔG_{compl} , ΔG_{r_off} and ΔG_{lig} . The results are in $kJ \cdot mol^{-1}$.

	Ligand	Complex	Binding
annihilation			
<i>atom, espp</i>	-1275.3 ± 11.2	1315.2 ± 16.3	8.6 ± 27.5
<i>atom, grom</i>	-1259.0 ± 5.9	1314.8 ± 13.2	24.5 ± 19.1
decoupling			
<i>atom, espp</i>	-151.9 ± 8.0	193.0 ± 9.1	9.8 ± 17.1
<i>aa-3, espp</i>	-151.9 ± 8.0	184.2 ± 14.4	1.0 ± 22.4
<i>aa-4, espp</i>	-151.9 ± 8.0	188.3 ± 15.3	5.1 ± 23.3
<i>aa-5, espp</i>	-151.9 ± 8.0	196.4 ± 8.5	13.2 ± 16.5
<i>aa-6, espp</i>	-151.9 ± 8.0	193.8 ± 7.8	10.6 ± 15.8
<i>aa-7, espp</i>	-151.9 ± 8.0	187.9 ± 4.8	4.7 ± 12.8
<i>aa-8, espp</i>	-151.9 ± 8.0	188.0 ± 5.1	4.8 ± 13.1
<i>aa-9, espp</i>	-151.9 ± 8.0	186.6 ± 10.3	3.4 ± 18.3
<i>aa-10, espp</i>	-151.9 ± 8.0	188.5 ± 3.5	5.3 ± 11.5

tiscale approach to model hydrogen bonding: The case of polyamide. *The Journal of Chemical Physics*, 142(22):224907, 2015.

- [11] Marilisa Neri, Claudio Anselmi, Michele Cascella, Amos Maritan, and Paolo Carloni. Coarse-grained model of proteins incorporating atomistic detail of the active site. *Phys. Rev. Lett.*, 95:218102, Nov 2005.
- [12] Marilisa Neri, Marc Baaden, Vincenzo Carnevale, Claudio Anselmi, Amos Maritan, and Paolo Carloni. Mi-

croseconds dynamics simulations of the outer-membrane protease t. *Biophysical Journal*, 94(1):71 – 78, 2008.

- [13] Matias Rodrigo Machado, Pablo Daniel Dans, and Sergio Pantano. A hybrid all-atom/coarse grain model for multiscale simulations of dna. *Phys. Chem. Chem. Phys.*, 13:18134–18144, 2011.
- [14] Matias R. Machado and Sergio Pantano. Exploring LacI–DNA dynamics by multiscale simulations using the sirah force field. *Journal of Chemical Theory and Computation*, 11(10):5012–5023, 2015. PMID: 26574286.
- [15] Aoife C. Fogarty, Raffaello Potestio, and Kurt Kremer. A multi-resolution model to capture both global fluctuations of an enzyme and molecular recognition in the ligand-binding site. *Proteins: Struct., Func., and Bioinf.*, 84(12):1902–1913, 2016.
- [16] Andrea Amadei, Antonius B. M. Linssen, and Herman J. C. Berendsen. Essential dynamics of proteins. *Proteins: Structure, Function, and Bioinformatics*, 17(4):412–425, 1993.
- [17] Vincenzo Carnevale, Simone Raugei, Cristian Micheletti, and Paolo Carloni. Convergent dynamics in the protease enzymatic superfamily. *J. Am. Chem. Soc.*, 2:173–181, 2006.
- [18] Andrea Zen, Vincenzo Carnevale, Arthur M. Lesk, and Cristian Micheletti. Correspondences between low-energy modes in enzymes: Dynamics-based alignment of enzymatic functional families. *Protein Sci.*, 17:918–929, 2008.
- [19] F. Pontiggia, A. Zen, and C. Micheletti. Small and large scale conformational changes of adenylate kinase: a molecular dynamics study of the subdomain motion and mechanics. *Biophys J*, 95(12):5901–5912, Dec 2008.
- [20] Monique M. Tirion. Large amplitude elastic motions in proteins from a single-parameter, atomic analysis. *Phys. Rev. Lett.*, 77:1905–1908, Aug 1996.
- [21] K. Hinsen. Analysis of domain motions by approximate normal mode calculations. *Proteins*, 33:417–429, 1998.
- [22] M Delarue and Y H Sanejouand. Simplified normal mode analysis of conformational transitions in dna-dependent polymerases: the elastic network model. *J Mol Biol*, 320(5):1011–1024, 2002.
- [23] C. Micheletti, P. Carloni, and A. Maritan. Accurate and efficient description of protein vibrational dynamics: comparing molecular dynamics and gaussian models. *Proteins*, 55(3):635–645, May 2004.
- [24] Tod D. Romo and Alan Grossfield. Validating and improving elastic network models with molecular dynamics simulations. *Proteins: Structure, Function, and Bioinformatics*, 79(1):23–34, 2011.
- [25] R. Potestio, F. Pontiggia, and C. Micheletti. Coarse-grained description of proteins’ internal dynamics: an optimal strategy for decomposing proteins in rigid subunits. *Biophys J*, 96, 2009.
- [26] H. Golhke and M. F. Thorpe. A natural coarse graining for simulating large biomolecular motion. *Biophysical Journal*, 91:2115–2120, 2006.
- [27] Zhiyong Zhang, Lanyuan Lu, Will G. Noid, Vinod Krishna, Jim Pfaendtner, and Gregory A. Voth. A systematic methodology for defining coarse-grained sites in large biomolecules. *Biophysical Journal*, 95(11):5073 – 5083, 2008.
- [28] Zhiyong Zhang, Jim Pfaendtner, Andrea Grafmiller, and Gregory A. Voth. Defining coarse-grained representations of large biomolecules and biomolecular complexes from

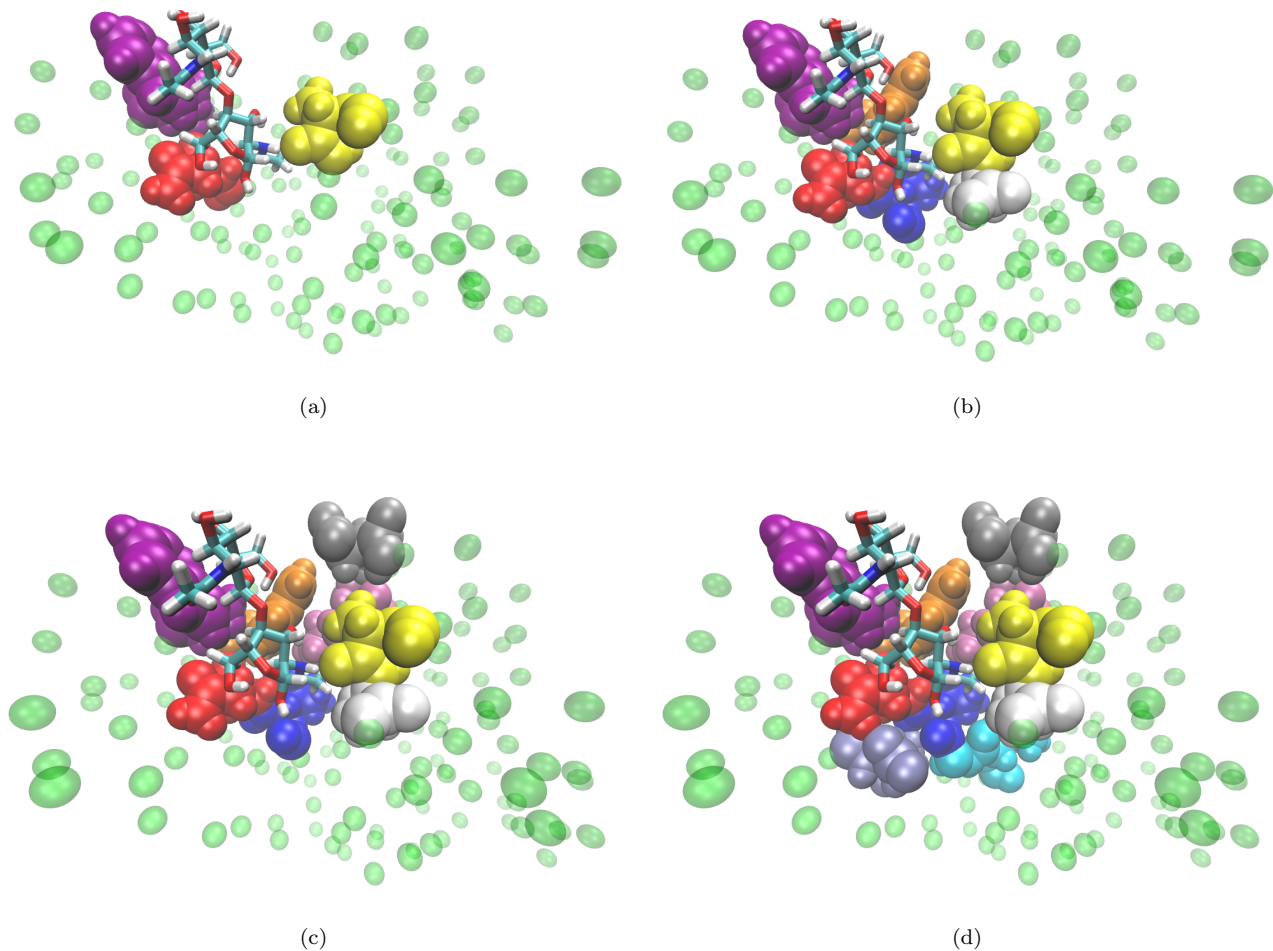


FIG. 5: VMD representation of lysozyme and ligand in different resolution: (a) three, (b) six, (c) eight, (d) ten atomistic residues. The complete set can be found in *Supporting information*. The ligand is always atomistic and it is represented in Licorice. In green are represented the ENM beads. With the other colors are represented, instead, the various atomistic residues which surround the ligand

elastic network models. *Biophysical Journal*, 97(8):2327–2337, 2009.

- [29] Zhiyong Zhang and Gregory A. Voth. Coarse-grained representations of large biomolecular complexes from low-resolution structural data. *Journal of Chemical Theory and Computation*, 6(9):2990–3002, 2010.
- [30] Anton V. Sinitskiy, Marissa G. Saunders, and Gregory A. Voth. Optimal number of coarse-grained sites in different components of large biomolecular complexes. *The Journal of Physical Chemistry B*, 116(29):8363–8374, 2012. PMID: 22276676.
- [31] Guido Polles, Giuliana Indelicato, Raffaello Potestio, Paolo Cermelli, Reidun Twarock, and Cristian Micheletti. Mechanical and assembly units of viral capsids identified via quasi-rigid domain decomposition. *PLoS Computational Biology*, 9(11):1–13, 11 2013.
- [32] Thomas T. Foley, M. Scott Shell, and W. G. Noid. The impact of resolution upon entropy and information in coarse-grained models. *The Journal of Chemical Physics*, 143(24):243104, 2015.
- [33] Patrick Diggins, Changjiang Liu, Markus Deserno, and Raffaello Potestio. Optimal coarse-grained site selection in elastic network models of biomolecules. *Journal of Chemical Theory and Computation*, 0(0):null, 0.
- [34] John G. Kirkwood. Statistical mechanics of fluid mixtures. *The Journal of Chemical Physics*, 3(5):300–313, 1935.
- [35] John D. Weeks, David Chandler, and Hans C. Andersen. Role of repulsive forces in determining the equilibrium structure of simple liquids. *The Journal of Chemical Physics*, 54(12):5237–5247, 1971.
- [36] M. Parrinello and A. Rahman. Polymorphic transitions in single crystals: A new molecular dynamics method. *Journal of Applied Physics*, 52(12):7182–7190, 1981.
- [37] Viktor Hornak, Robert Abel, Asim Okur, Bentley Strockbine, Adrian Roitberg, and Carlos Simmerling. Comparison of multiple amber force fields and development of improved protein backbone parameters. *Proteins: Struc-*

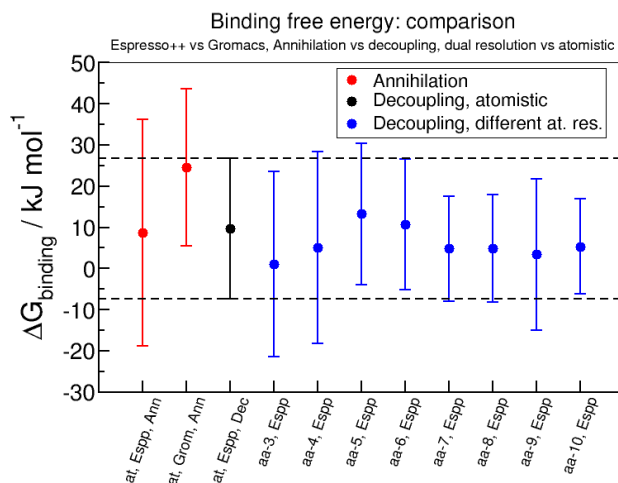


FIG. 6: Binding free energies as a function of protein’s residues included in atomistic detail in the multi-resolution set-up or fully atomistic set-up. The heavy dashed black horizontal lines and black point are the reference values from fully atomistic simulations obtained in ESPResSo++ with decoupling, and the lighter dotted black horizontal lines are the error bars for those values. In red are represented binding free energies values in ESPResSo++ and GROMACS in case of annihilation. In blue is represented the binding FE value in dual resolution simulation changing the number of atomistic residues.

ture, *Function, and Bioinformatics*, 65(3):712–725, 2006.

- [38] William L. Jorgensen, Jayaraman Chandrasekhar, Jeffrey D. Madura, Roger W. Impey, and Michael L. Klein. Comparison of simple potential functions for simulating liquid water. *The Journal of Chemical Physics*, 79(2):926–935, 1983.
- [39] Karl N. Kirschner, Austin B. Yongye, Sarah M. Tschampel, Jorge Gonzalez-Outeirio, Charlisa R. Daniels, B. Lachele Foley, and Robert J. Woods. Glycam06: A generalizable biomolecular force field. *carbohydrates. Journal of Computational Chemistry*, 29(4):622–655, 2008.
- [40] Mark Abraham, Berk Hess, David van der Spoel, and Erik Lindahl. The gromacs development team, gromacs user manual version 5.0.4. 2014.
- [41] Michael R. Shirts, Jed W. Pitera, William C. Swope, and Vijay S. Pande. Extremely precise free energy calculations of amino acid side chain analogs: Comparison of common molecular mechanics force fields for proteins. *The Journal of Chemical Physics*, 119(11):5740–5761, 2003.
- [42] Shuichi Miyamoto and Peter A. Kollman. Settle: An analytical version of the shake and rattle algorithm for rigid water models. *Journal of Computational Chemistry*, 13(8):952–962, 1992.
- [43] Hans C Andersen. Rattle: A “velocity” version of the shake algorithm for molecular dynamics calculations. *Journal of Computational Physics*, 52(1):24 – 34, 1983.
- [44] J.D.Halverson, T.Brandes, O.Lenz, A.Arnold, S.Bevc, V.Starchenko, K.Kremer, T.Stuehn, and D.Reith. Espresso++: A modern multiscale simulation package for soft matter systems. *Computer Physics Communications*, 184:1129–1149, 2013.
- [45] Horacio V. Guzman, Nikita Tretyakov, Hideki Kobayashi, Aoife C. Fogarty, Karsten Kreis, Jakub Krajniak, Christoph Junghans, Kurt Kremer, and Torsten Stuehn. Espresso++ 2.0: Advanced methods for multiscale molecular simulation. *Computer Physics Communications*, 238:66 – 76, 2019.
- [46] Berk Hess, Carsten Kutzner, David van der Spoel, and Erik Lindahl. Gromacs 4: Algorithms for highly efficient, load-balanced, and scalable molecular simulation. *Journal of Chemical Theory and Computation*, 4(3):435–447, 2008. PMID: 26620784.
- [47] Student. The probable error of a mean. *Biometrika*, 6(1):1–25, 1908.